PHYSICAL REVIEW B **82**, 020407(R) (2010)

Hysteretic synchronization of nonlinear spin-torque oscillators

Phillip Tabor
Department of Physics, West Virginia University, Morgantown, West Virginia 26506, USA

Vasil Tiberkevich and Andrei Slavin
Department of Physics, Oakland University, Rochester, Michigan 48309, USA

Sergei Urazhdin
Department of Physics, West Virginia University, Morgantown, West Virginia 26506, USA

(Received 24 June 2010; published 23 July 2010)

We report the observation of hysteretic synchronization of point-contact spin-torque nano-oscillators by a microwave magnetic field. The hysteresis is asymmetric with respect to the frequency detuning of the driving signal and appears in the region of a strong dependence of the oscillation frequency on the bias current. Theoretical analysis shows that hysteretic synchronization occurs when the width of the synchronization range, enhanced by the oscillator's nonlinearity, becomes comparable to the dissipation rate, while the observed asymmetry is a consequence of the nonlinear dependence of frequency on the bias current. Hysteretic synchronization is a general property of strongly nonlinear oscillators, and can therefore be expected to affect the dynamics of a variety of physical systems.

DOI: 10.1103/PhysRevB.82.020407 PACS number(s): 76.50.+g, 05.45.Xt, 75.75.Jn, 85.70.Ec

Among the auto-oscillating systems, the class of nonlinear (or nonisochronous) auto-oscillators is characterized by a strong dependence of their frequency ω_0 on the oscillation power p.[1–3] When such an oscillator is driven by a periodic force, its nonlinearity can enhance the range of synchronization. This effect results from the reduction in the detuning between ω_0 and the frequency ω_e of the driving force, caused by the variations of p.[2,3]

The nonlinearity can also have a *qualitative* effect on the dynamical properties of the oscillator. In quasilinear auto-oscillating systems, synchronization can be described by Adler's phase equation[2,4] and the synchronization transition is interpreted as the simultaneous creation of a stable node and a saddle point, which is a nonhysteretic process. In contrast, for nonisochronous oscillators such as magnetic spin-torque nano-oscillators (STNO),[5–8] analysis that includes variations of both the phase and the amplitude indicates that periodic and quasiperiodic states can remain simultaneously stable, resulting in *hysteretic* synchronization.[9] This predicted but previously unobserved effect is qualitatively different from the well-known hysteretic transition between different synchronization regimes,[2] which is caused by the coexistence of multiple stable synchronized states and does not require nonlinearity. Understanding the synchronization properties of STNO may be important for the application of STNO arrays as microwave sources with enhanced generation characteristics.[7,10–16]

Here, we report the observation of hysteretic synchronization of a point-contact STNO to an external periodic signal provided by a large microwave magnetic field, enabled by a device geometry incorporating a nanoscale microwave antenna. The hysteresis is observed in the region where the auto-oscillation frequency exhibits a strong dependence on the bias current, confirming the correlation of this phenomenon with the nonlinear properties of the oscillator. The hysteretic synchronization is *asymmetric*, i.e., at each value of the bias current the hysteresis generally occurs only at the lower or the upper frequency boundary of the synchronization range, and in this respect is different from the symmetric hysteresis predicted in Ref. 9. Our analysis based on a *generic* model of a nonlinear auto-oscillator suggests that the phenomenon of hysteretic synchronization is not specific to STNO, but is rather a *general property* of nonlinear auto-oscillators, independent of their physical nature.

Devices with structure

$$\mathrm{Cu(40)Py(3.5)Cu(8)Co_{70}Fe_{30}(10)Cu(60)}$$

were fabricated on sapphire substrates patterned into coplanar striplines, by a procedure described elsewhere.[17] All thicknesses are in nanometers, $\mathrm{Py=Ni_{80}Fe_{20}}$. The polarizing CoFe layer was patterned into a 100 nm $\times$ 50 nm nanopillar while the free Py(3.5) layer was left extended with dimensions of several micrometers [Fig. 1(a)], thus forming a device geometry similar to the magnetic point contact studied in Ref. 8. Magnetic oscillations of the Py layer in the point-contact area were induced by a dc bias current $I_0>0$ flowing from CoFe. We also performed measurements in a more common device geometry with a nanopatterned free layer but have not observed hysteresis in these devices, likely due to the smaller nonlinearity and stronger effects of fluctuations that generally suppress hysteretic phenomena.

In all the previous measurements of synchronization in STNO, the external driving signal was provided by an ac current superimposed on the dc bias current.[10,18,11] In contrast, in our experiments the driving signal was provided by a microwave magnetic field, enabling us to achieve significantly stronger driving. The microwave field was generated by a 300-nm-wide and 250-nm-thick Cu microstrip fabricated on top of the STNO, and electrically isolated from it by a $SiO_2(50)$ layer [Fig. 1(a)]. The microstrip was oriented at 45° with respect to the nanopillar easy axis. To calibrate the

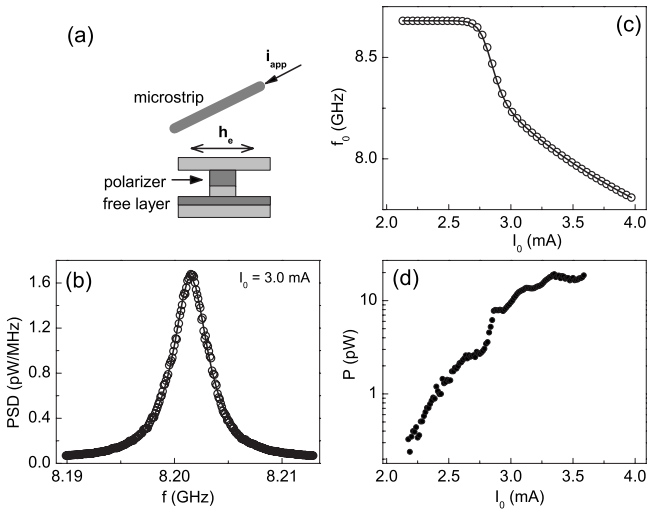

FIG. 1. (a) Schematic of the device including an STNO and a microstrip line generating a synchronizing Oersted field. (b) Example of auto-oscillation spectrum at I_0=3 mA (symbols) and Lorentzian fitting with full width at half maximum of 4 MHz (solid curve). (c) Symbols: auto-oscillation frequency vs bias current. Curve: our model fitting, as described in the text. (d) Emitted power under the oscillation peak vs bias current.

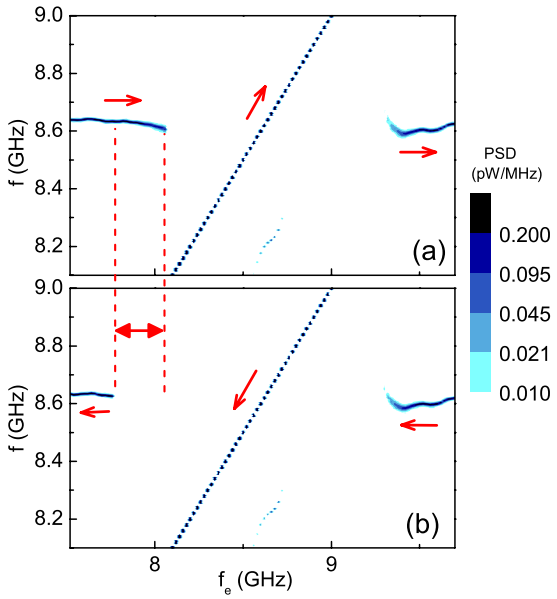

FIG. 2. (Color online) Dependence of the oscillation frequency f of STNO on the driving frequency f_e, demonstrating hysteretic synchronization to the external signal: (a) increasing f_e and (b) decreasing f_e, at I_0=2.7 mA. The bias field H_0 is perpendicular to the microwave driving field h_e=18 Oe. Arrows show the direction of the scan and dashed vertical lines show the limits of the hysteretic synchronization range; a double arrow shows the width of the hysteresis interval.

Oersted field h_e produced by the microstrip, we compared the dependence of the auto-oscillation frequency f_0 on the dc bias field H_0 to the dependence of f_0 on the dc current i_{app} applied to the microstrip with H_0 oriented perpendicular to the direction of the microstrip, yielding h_e (Oe)=9.0 i_{app} (mA). The frequency-dependent microwave losses were determined by utilizing a separately fabricated transmission line with the same microstrip geometry. These losses were taken into account when determining the microwave Oersted field generated by the microstrip. Loss-adjusted ac currents of up to 4 mA rms were applied to the microstrip without noticeable heating, producing h_e of up to 36 Oe rms at the location of the STNO.

Microwave signals applied to the microstrip produced parasitic currents in STNO in addition to the Oersted field. In our measurements, the parasitic coupling did not exceed −25 dB, inducing microwave currents of less than 12 μA rms at the largest driving amplitude. As demonstrated below, the effects of these parasitic currents on the oscillation are smaller than those of the microwave field. All the measurements were performed at 5 K, at a dc bias field H_0=1.1 kOe. The reported results were confirmed for two devices.

Magnetic static and dynamical characteristics of STNO were determined by measurements of magnetoresistance and auto-oscillation spectra. The auto-oscillation spectra had a Lorentzian lineshape with a typical full width at half maximum of 4 MHz, consistent with the effects of thermal broadening[3,19,20] [Fig. 1(b)]. Above the oscillation onset at bias current I_t=2.0 mA, the frequency f_0 of the auto-oscillation was initially approximately constant. At I_0>2.75 mA, it exhibited a region of strong redshifting with a gradually decreasing slope df_0/dI_0 [Fig. 1(c)]. This redshifting region is correlated with the increase in the slope in the dependence of the emitted power on the bias current [Fig. 1(d)]. A similar transition from a nearly constant frequency to a strongly redshifting behavior was observed in the other studied device. In both samples, hysteresis was observed in the vicinity of this strong frequency redshift.

Parasitic coupling produced peaks at $f=f_e$ in spectroscopic measurements of driven oscillations, regardless of the oscillation regime. Therefore, the transition to the synchronized regime was identified as an abrupt disappearance of the $f_0 \approx$ const. line of unlocked oscillation (Fig. 2). Note that the frequency pulling, which is a general feature of synchronization in linear oscillators, is negligible in the data of Fig. 2. The frequency at the lower boundary of the detuning interval in the synchronized regime is larger by 0.31 GHz for f_e scanned up [Fig. 2(a)] than for f_e scanned down [Fig. 2(b)], demonstrating hysteretic synchronization.

The synchronization range and the hysteresis were significantly larger for $H_0 \perp h_e$ than for $H_0 \| h_e$, confirming the dominance of the effects of the microwave field over the parasitically induced microwave current [Figs. 3(a) and 3(b)]. A similar dependence of hysteresis on the field orientation was also observed in the other tested device. These data explain why hysteresis has not been previously observed in measurements of synchronization induced by a microwave current. Indeed, in a typical geometry of spin transfer devices, the current polarization is nearly collinear with the static magnetization of the free layer. In this case, the synchronization effects are similar to those of $h_e \| H_0$ in Fig. 3(b), producing only a small hysteresis. A driving microwave current with polarization *perpendicular* to the magnetization of the free layer would likely produce a large hys-

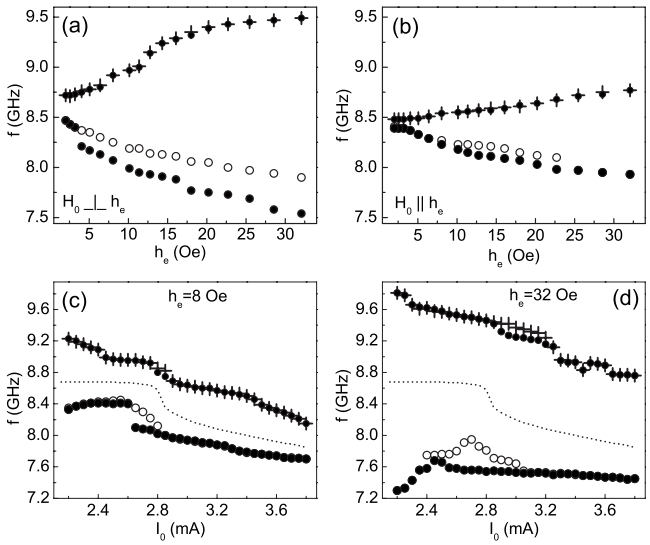

FIG. 3. (a) Dependence of the synchronization boundaries on the rms amplitude h_e of the driving microwave magnetic field, for $H_0 \perp h_e$ at $I_0=2.7$ mA. Crosses: upper synchronization boundary for f_e scanned up, dots: upper synchronization boundary for f_e scanned down, open circles: lower synchronization boundary for f_e scanned up, and solid circles: lower synchronization boundary for f_e scanned down. (b) Same as (a), for $H_0 \| h_e$. (c) Dependence of the synchronization boundaries on the bias current I_0, at $h_e=8$ Oe perpendicular to H_0. Dashed curves show the auto-oscillation frequency. (d) Same as (c), at $h_e=32$ Oe.

teresis, similar to our geometry with $h_e \perp H_0$. However, such a geometry would not allow excitation of auto-oscillations via the spin transfer effect.[21] In addition, Figs. 3(a) and 3(b) demonstrate that hysteresis appears only above a certain threshold driving amplitude, which may not have been achieved in the published measurements of synchronization by microwave current.

Measurements of the dependence of the synchronization on I_0 indicate that the hysteretic behaviors are correlated with the nonlinear characteristics of the auto-oscillation. At a small driving field $h_e=8$ Oe [Fig. 3(c)], the hysteresis appears at the lower boundary of the synchronization range at $2.65\ \text{mA} \leq I_0 \leq 2.8$ mA, i.e., close to the region where the auto-oscillation (dashed curve) exhibits the largest frequency redshift. A small hysteresis is also observed at the upper boundary of the synchronization range at $I_0=2.8-2.85$ mA. At a larger driving amplitude $h_e=32$ Oe [Fig. 3(d)], the synchronization interval and the magnitude of hysteresis increase and hysteretic synchronization is observed over a larger range of bias currents. The hysteresis at the upper boundary of the synchronization interval remains small, but occurs over a broad range of I_0 from 2.85 to 3.2 mA. The observed asymmetry of hysteresis was confirmed in both tested devices for several values of the bias field.

Our experimental results confirm the prediction of synchronization hysteresis made by Bonin *et al.*[9] The primary distinction between the predicted behaviors and our results is the observation of a strong asymmetry with respect to the sign of frequency detuning. To understand the origin of the asymmetry, we performed numerical simulations of synchronization taking into account the strong nonlinear dependence of the auto-oscillation frequency on the bias current. Our simulations were based on the nonlinear auto-oscillator model[3] for the complex oscillation amplitude $c(t)$

$$\frac{dc}{dt} + i\omega_0(p)c + [\Gamma_0 - \sigma I_0(1-p)]c = \gamma h_e e^{-i\omega_e t}. \qquad (1)$$

Here, γ is the gyromagnetic ratio, $p=|c|^2$ is the dimensionless precession power, $\omega_0(p)$ is the auto-oscillation frequency, Γ_0 is the natural positive magnetic damping, which for simplicity is assumed independent of p. The parameter σ was defined by Eq. (4b) in Ref. 3, such that $\sigma I_0(1-p)$ is the negative damping induced by the spin transfer. The right-hand side of Eq. (1) represents the action of the driving microwave magnetic field of amplitude h_e and frequency ω_e. For simplicity, we neglect the ellipticity of the magnetization precession. This assumption is equivalent to an effective renormalization of the driving amplitude h_e and does not qualitatively modify the results. The driving field is oriented orthogonal to the magnetization precession axis to model the experimental geometry exhibiting the largest hysteresis.

The coefficient σ in the linear relationship between the current and the spin torque is determined predominantly by the spin-polarization efficiency of the polarizing layer. We chose $\sigma=2.0\ \text{ns}^{-1}\ \text{mA}^{-1}$, which corresponds to the dimensionless spin-polarization efficiency $\varepsilon \simeq 0.4$. The damping rate Γ_0 is determined by a combination of the Gilbert damping ($\alpha \simeq 0.01$) and radiative damping due to spin wave propagation away from the area of the nanocontact. In our simulations, we chose $\Gamma_0=4.0\ \text{ns}^{-1}$ to reproduce the experimental value of the auto-oscillation onset current $I_t=\Gamma_0/\sigma=2.0$ mA. The dependence of the power of the stationary auto-oscillation on the bias current was calculated from Eq. (1) as $p_0=(I_0-I_t)/I_0$.

The adequacy of our model for the analysis of hysteretic synchronization was initially verified by assuming a linear relationship between the oscillation frequency and bias current, similar to the model of Bonin *et al.* In this approximation, our simulations yielded symmetric hysteresis consistent with the results of Ref. 9. To model the effect of the actual nonlinear properties of our devices, we analyzed the experimental relationship [Fig. 1(c)] between of the auto-oscillation frequency and the bias current, yielding the dependence $\omega_0(p)$ of the frequency on the power of the oscillator, without any additional assumptions. We fitted this dependence by $\omega_0(p)=54.5+(1.16-7.85p)[1+\tanh(38.5p-11.3)]$, where ω_0 is expressed in ns^{-1}, which provides an excellent approximation for the experimental data [Fig. 1(c)].

Figure 4(a) shows an example of the simulated synchronization at $I_0=2.4$ mA, $h_e=30$ Oe, for two opposite directions of the driving frequency sweep. The simulation exhibits a significant hysteresis only at the lower synchronization boundary. In addition, the unlocked oscillation frequency remains constant up to the synchronization transition, i.e., the frequency pulling is negligible. Both of these features are in remarkable agreement with the experiment (Fig. 2).

The simulated dependence of synchronization on the bias current is consistent with the most prominent features of the experimental data, as illustrated in Fig. 4(b) for $h_e=30$ Oe.

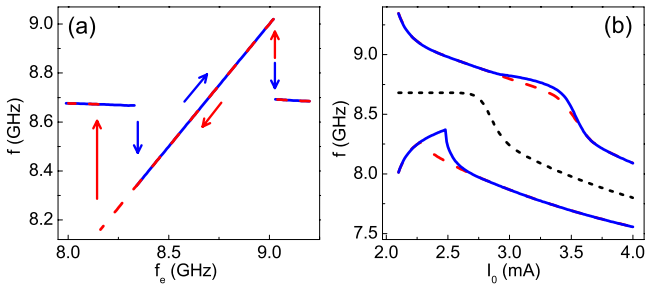

FIG. 4. (Color online) (a) Numerical simulations of the STNO synchronization with increasing (blue solid curve) and decreasing (red dashed curve) driving frequency f_e at I_0=2.4 mA, h_e=30 Oe. (b) Calculated dependence of the synchronization limits on I_0 for h_e=30 Oe. Black dotted curve shows the free running frequency.

In our simulations, the synchronization hysteresis appeared at $h_e > h_t \approx 15$ Oe, when the width of the synchronization interval, which is proportional to h_e and is enhanced by the oscillator's nonlinearity,[2,3] becomes comparable to the auto-oscillator dissipation rate Γ_0. Additional simulations performed for different values of Γ_0 showed that the hysteresis generally appears at driving field amplitudes exceeding the threshold value determined by $\Delta f_e \approx \Gamma_0/(2\pi)$. Thus, measurements of the synchronization range for $h_e \approx h_t$ can be used to determine the dissipation rate Γ_0 of a nonlinear auto-oscillator.

At h_e=30 Oe above the excitation threshold [Fig. 4(b)], the simulated synchronization exhibits a large hysteresis at the lower synchronization boundary, at currents below the point of the maximum slope $|d\omega_0(p)/dp|$. A small hysteresis also appears at the upper synchronization boundary over a broad range of the bias current, above the point of the maximum slope $|d\omega_0(p)/dp|$. These features are in excellent agreement with the experimentally observed behaviors, confirming that the observed asymmetry of the hysteresis is caused by the strong nonlinearity of the dependence of the auto-oscillation frequency on the oscillation power.

In summary, we have demonstrated the predicted hysteretic synchronization of a nonlinear magnetic nano-oscillator by a microwave magnetic field. Our observations indicate that the hysteresis is correlated with the region of large nonlinear red frequency shift, linking the phenomenon of hysteresis to the nonlinearity of the oscillator. Simulations based on the model of strongly nonlinear auto-oscillator, taking into account the observed dependence of frequency on the bias current, yielded good semiquantitative agreement with the most salient features of the experiment. The subtle dependence of hysteretic synchronization on the nonlinear properties of the oscillator can be utilized to extract important information about the dynamical characteristics of spin torque nano-oscillators, as well as other strongly nonlinear oscillating systems.

This work was supported by NSF under Grants No. DMR-0747609 and No. ECCS-0653901, the Research Corporation, U.S. Army TARDEC, RDECOM (Contract No. W56HZV-09-P-L564), and Oakland University Foundation.

[1] A. Blaquiere, *Nonlinear System Analysis* (Academic, New York, 1966).
[2] A. Pikovsky, M. Rosenbblum, and J. Kurths, *Synchronization: A Universal Concept in Nonlinear Sciences* (Cambridge University Press, New York, 2001).
[3] A. Slavin and V. Tiberkevich, IEEE Trans. Magn. **45**, 1875 (2009).
[4] R. Adler, Proc. IRE **34**, 351 (1946).
[5] J. Slonczewski, J. Magn. Magn. Mater. **159**, L1 (1996).
[6] L. Berger, Phys. Rev. B **54**, 9353 (1996).
[7] S. I. Kiselev, J. C. Sankey, I. N. Krivorotov, N. C. Emley, R. J. Schoelkopf, R. A. Buhrman, and D. C. Ralph, Nature (London) **425**, 380 (2003).
[8] W. H. Rippard, M. R. Pufall, S. Kaka, S. E. Russek, and T. J. Silva, Phys. Rev. Lett. **92**, 027201 (2004).
[9] R. Bonin, G. Bertotti, C. Serpico, I. D. Mayergoyz, and M. d'Aquino, Eur. Phys. J. B **68**, 221 (2009).
[10] W. H. Rippard, M. R. Pufall, S. Kaka, T. J. Silva, S. E. Russek, and J. A. Katine, Phys. Rev. Lett. **95**, 067203 (2005).
[11] B. Georges, J. Grollier, M. Darques, V. Cros, C. Deranlot, B. Marcilhac, G. Faini, and A. Fert, Phys. Rev. Lett. **101**, 017201 (2008).
[12] S. Kaka, M. R. Pufall, W. H. Rippard, T. J. Silva, S. E. Russek, and J. A. Katine, Nature (London) **437**, 389 (2005).
[13] F. B. Mancoff, N. D. Rizzo, B. N. Engel, and S. Tehrani, Nature (London) **437**, 393 (2005).
[14] D. C. Ralph and M. D. Stiles, J. Magn. Magn. Mater. **320**, 1190 (2008).
[15] D. V. Berkov and J. Miltat, J. Magn. Magn. Mater. **320**, 1238 (2008).
[16] T. J. Silva and W. H. Rippard, J. Magn. Magn. Mater. **320**, 1260 (2008).
[17] S. Urazhdin and P. Tabor, J. Appl. Phys. **105**, 066105 (2009).
[18] J. C. Sankey, P. M. Braganca, A. G. F. Garcia, I. N. Krivorotov, R. A. Buhrman, and D. C. Ralph, Phys. Rev. Lett. **96**, 227601 (2006).
[19] J. C. Sankey, I. N. Krivorotov, S. I. Kiselev, P. M. Braganca, N. C. Emley, R. A. Buhrman, and D. C. Ralph, Phys. Rev. B **72**, 224427 (2005).
[20] V. S. Tiberkevich A. N. Slavin, and Joo-Von Kim, Phys. Rev. B **78**, 092401 (2008).
[21] F. B. Mancoff, R. W. Dave, N. D. Rizzo, T. C. Eschrich, B. N. Engel, and S. Tehrani, Appl. Phys. Lett. **83**, 1596 (2003).